The Art of Signal Reception: Practical Interference Alignment

Milad Johnny and Alireza Vahid

Abstract

We present a new receiver antenna hardware structure as well as a new communication protocol to effectively remove most of the interference signal power in K-user interference channels. In particular, we present a new blind interference alignment technique alongside the necessary hardware for its practical implementation. The proposed hardware is a reconfigurable patch antenna in which each patch can be controlled individually to create huge diversity at the receiver. The goal is to find two separate combinations of activating or deactivating patches to allow for interference neutralization/alignment. Finding such states is a cumbersome task for which we develop low-complexity efficient algorithms. Finally, we devise simple encoding and decoding with short pre-coder length to exploit the benefits of our hardware design. Our implementation does not rely on channel state information at the transmitters; works at finite signal-to-noise ratios unlike the typical degrees-of-freedom results; and works in slow-fading environments. We demonstrate how our approach can reduce the effect of interference signals in a multi-path environment, we calculate the average achievable rates, and we provide outage analysis of our technique. We also evaluate the complexity of our technique and present an efficient solution.

Index Terms

Blind interference alignment, average sum rate, outage capacity, integer programming, reconfigurable antenna.

I. Introduction

The interference channel (IC) models single-hop peer-to-peer communication, and many wireless networks, such as cellular networks in which base stations communicate to mobile users, fall under this model. Other wireless networks such as microcells and femtocells can be also

Alireza Vahid is with the department of Electrical Engineering at the University of Colorado Denver, USA. Authors' email addresses: mjohnny@uwaterloo.ca and alireza.vahid@ucdenver.edu.

modeled as interference channels. In fact, moving towards denser networks and more aggressive spectrum reuse accentuates the importance of interference channels in which network capacity improvement is hampered by the interference signal power.

Unfortunately, except for special cases [1]–[3] the capacity of interference channel networks remains unknown. Broadly speaking, the Han-Kobayashi scheme [4] which uses rate splitting is considered to be the best achievable scheme for two-user interference channels. Especially for a class of injective deterministic interference channels, the optimality of this approach using converse proof has been demonstrated [5]. But for more than two users and for other types of interference channels, this approach does not scale. Therefore, the problem of interference in many wireless networks continues to limit network capacity and any practical interference management solution would be of great importance.

A commonly used method for handling interference is to simply avoid the problem through orthogonalization such as time-frequency division medium access (TDMA) or code division medium access (CDMA). Unfortunately, these schemes are suboptimal and cannot support the increasing demand for higher communication data rates. Another approach to improve spectral efficiency is to use multiple antenna structures and to use joint processing at the receivers which require channel state information at the transmitters. To complement the previous approach, several results explore using multiple antenna structures at the receivers which require joint processing at the receivers, several RF chains in the design, and multi-channel ADC. These characteristics add significant hardware complexity [6].

In recent years, the concept of interference alignment (IA) has been proposed as a more sophisticated form of interference management. In the context of K-user interference channels, IA achieves a sum degrees-of-freedom (DoF) of $K/2$. DoF is the pre-log factor in the expression for achievable rates and can be thought of as the equivalent number of parallel point-to-point additive white Gaussian noise (AWGN) channels inside a larger network when the signal-to-noise ratio (SNR) tends to infinity. In other words, IA shows that the number of interference-free dimensions scales linearly with the number of users. Thus, a $K/2$ DoF exhibits significant improvement over orthogonalization techniques which only achieve a DoF of 1. Although IA has a lot of theoretical benefits, there are a number of challenges and barriers in translating this method into a practical solution such as the assumption of high-resolution CSI (in some cases global perfect CSI) for the $K-$user IC, the fast-fading channel model, and long precoder lengths at the transmitters [7], [8]. These challenges cast doubt about the practicality of the IA concept.

There are different approaches to reducing the sensitivity of interference alignment to CSI. The first one is related to accessing CSI within limited distortion [9], the second one is related to delayed CSI [10]–[14], and finally, the last one is known as blind IA (BIA) [15], [16]. The latter is the main focus of this paper. The authors in [17], [18] show that in the case of blind channel knowledge or even finite precision CSI, the sum DoF of interference channel collapses to what is achievable by time or frequency sharing methods. However, this rather discouraging observation, as we show in this paper, does not mean that no gain can be obtained at finite SNR. In fact, we show that we can fully trace the $K/2$ scaling factor within some operation SNR range.

In [15], the authors show that if the channel coherence has some specific structure, then the benefits of IA can be still attained without accessing CSI at the transmitters. To control channel coherence times, one idea is to use multi-mode switching antennas at the receivers [19], [20]. In this case, the receivers are equipped with an antenna that can switch among r different reception modes and the transmitters use specifically designed precoders to create the transmission signals. Using this approach, a sum DoF of $6/5$ is achievable in 3-user ICs. This approach is also generalized to $K-$user interference channels to show that when the number of users goes to infinity, the sum DoF goes to the value of $\sqrt{K}/2$ [16].

In [20] and with much more practical insights in [21], the authors propose a method to implement IA in a multipath fading environment. The key element is a new antenna structure that creates huge diversity gain and proper channel conditions to align (most of) the interference signal power. However, the complexity of the designs and the algorithms limit the practicality of the results.

In this paper, the key insight is to focus on receiver diversity for interference management, and design appropriate hardware and physical-layer protocols to eliminate the interference power. More specifically, we propose a new antenna structure with several sub-elements that can be controlled individually using RF switches. The antenna structure is designed such that it can generate a large number of reception states. Among these reception states, some will be amenable to the interference management strategy we propose in this paper, and we refer to such states as "proper channel conditions". We quantify the relationship between the number of sub-elements and the chance for finding proper channel conditions at the receivers, and we propose an efficient search algorithm to find them. Once these states are identified, transmitters follow a simple transmission protocol and at the receivers, using the proposed antenna structure, interfering

signals are (mostly) eliminated. We calculate the average achievable sum rate, provide outage analysis, and theoretically evaluate the distribution of the reception gain of the receiver antenna for each combined switching state. We show that it is possible to measure only a small number of reception sates in order to calculate the entire space at each receiver. We quantify the trade-off between the achievable rates and the complexity of different algorithms. More specifically, increasing the number of antenna sub-elements, increases the chance of interference alignment conditions, but increases the complexity of the search algorithm at the same time, and we quantify this trade-off.

In Section II, we introduce the system model, receiver antenna structure, and some preliminaries as well as a motivating example. In Section IV, we provide a detailed motivation for our work, some notes on our results vis-a-vis existing literature, and an overview of our contributions. We present the relation between the minimum number of antenna sub-elements and average transmission rate in Section V, and we also analyze the outage capacity behaviour of our network for each user in this section. We propose a search algorithm in Section VI, and we demonstrate how to find proper channel states at each receiver, and we analytically evaluate the complexity of our search algorithm. We present our numerical and simulation results in Section VII. Finally, Section VIII concludes the paper.

II. System Model and Proposed Receiver Antenna Structure

In this paper, we consider a multi-cell communication system modeled as a K-user interference channel with no cooperation among the transmitters. In other words, transmitters do not exchange any data with each other. All the transmitters equipped with a simple antenna that can be used for today wireless networks, such as Omni-directional or directional antennas to have more transmission gain and lower interference generation for a local reception zone. We assume that each receiver is equipped with an antenna structure we propose in this paper.

A. Antenna Structure

The proposed antenna structure consists of M sub-elements and one RF chain which as depicted in Fig. 1a.

Remark 1: In our proposed system and protocol, no joint processing is performed at the receivers, and the antenna structure does not have the typical hardware and software complexity

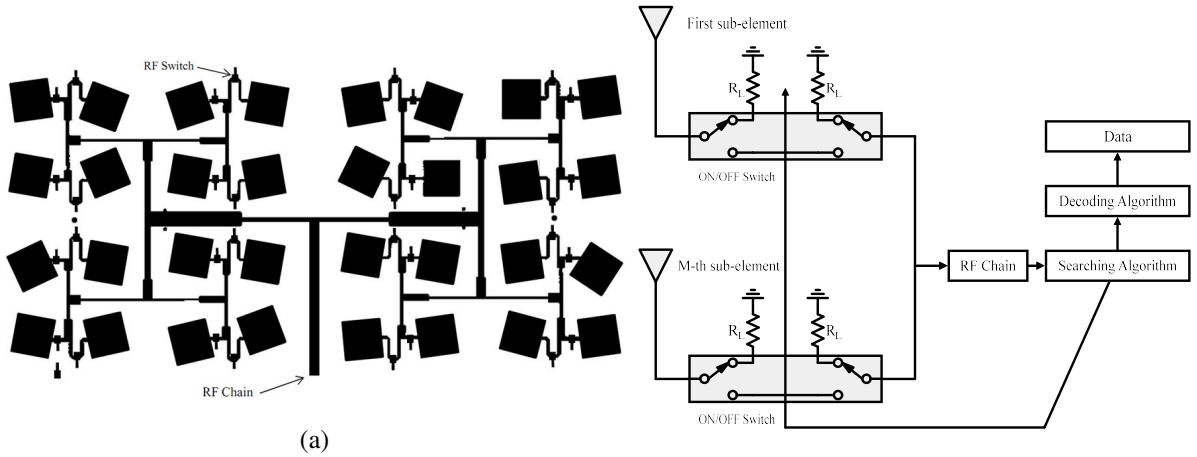

(a) (b)

Fig. 1: (a) Receiver patch antenna structure with random orientations alongside RF combiners and RF switches; (b) the receiver can control the reception mode of its antenna.

of multiple input antenna structures used in single-input multiple-output (SIMO) and multiple-input multiple-output (MIMO) transceivers. We further note that the antenna is not used for receiver beamforming. As we discuss later, we benefit from the multipath characteristics of the environment, something beamforming does not capitalize on.

In the proposed antenna structure, each sub-element is semi-randomly[1] oriented to add spatial diversity in the received signal. The receiver can control these elements using M separate RF switches.Therefore, the receiver can control these RF switches to scan through and to create 2^M different reception states. Further, in the receiver antenna, all elements are connected to a power combiner using RF switches. Basically, the role of these RF switches is to connect the power combiner network to each of the elements or to a match load. When an RF switch is in the active state, the power combiner network is connected to its corresponding element and it can receive RF signal from the environment. When an RF switch is in the inactive mode, the power combiner network and antenna subelement are connected to a passive match load (R_L), and the power combiner is disconnected from environmental signals, see Fig. 1b. All sub-elements are connected through a power combiner, the signals are filtered, amplified, and down-converted using a single RF chain as in Fig. 1b. Thus, there is no need to implement several RF chains in the proposed structure.

[1]Ideally, the elements are randomly oriented, but hardware and structural limitations result in semi-randomly designs.

Each element of the receiver antenna has a random orientation with the reception gain of $A(\theta-\theta_i, \phi-\phi_i)$, $1 \leq i \leq M$, where θ_i and ϕ_i indicate the angular position of each element and variables θ and ϕ indicate the reception gain dependence on the direction from each element of the antenna.

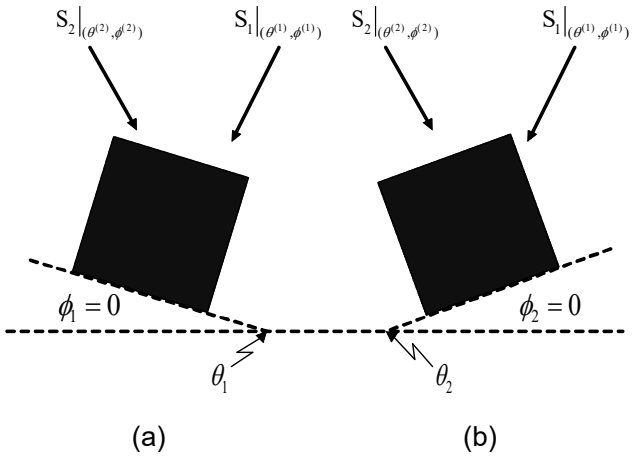

Fig. 2: Two separate sub-elements of the receiver antenna with random orientation.

For our antenna structure, since all sub-elements are on the same plane, all of them have the same elevation orientation angle. In other words, we have:

$$\phi_1 = \phi_2 = \cdots = \phi_M, \tag{1}$$

but each sub-element has a random azimuth orientation angle. As an example, in Fig. 2 two receiver sub-elements with random orientations of θ_1 and θ_2 have been depicted. The receive signal is the function of antenna orientation angle, for Fig. 2(a), the received signal has the following form:

$$A(\theta_1 - \theta^{(1)}, \phi^{(1)})S_1 + A(\theta_1 - \theta^{(2)}, \phi^{(2)})S_2, \tag{2}$$

and for Fig. 2(b), the received signal is:

$$A(\theta_2 - \theta^{(1)}, \phi^{(1)})S_1 + A(\theta_2 - \theta^{(2)}, \phi^{(2)})S_2, \tag{3}$$

and these equations are linearly independent. Therefore, random orientation of each element leads to generation of different linear combinations of the received signals. In a real scenario, we have multiple received signal paths which generates many different reception signal gains for different antenna sub-elements.

Role of the proposed antenna: The goal of the proposed antenna structure is to find some proper states to align the interfering signals in a subspace which is linearly independent of the desired signal. Implementing this reception structure can drastically increase the transmission rate without channel state information at the transmitters. Fig. 3 shows an interference network with of 3 users in which receivers are equipped with the proposed structure each with $M = 8$ sub-elements.

B. System Model

We consider a $K-$user interference channel (IC) with K transmitters TX_k, and K receivers $\mathrm{RX}_k, k \in \mathcal{K} = \{1, \ldots, K\}$. Each receiver is equipped with the antenna structure described in the previous subsection. Each element of the receiver antenna receives a signal from all of the transmitters. In Fig. 1a, each receiver antenna consisted of $M = 32$ squared patch elements which are connected using 32 switches and a power combiner. We can model the reception state of each receiver antenna by $M-$tuple of $S^{[j]} = (s_1^{[j]}, \ldots, s_M^{[j]}), s_i \in \{0, 1\}$.

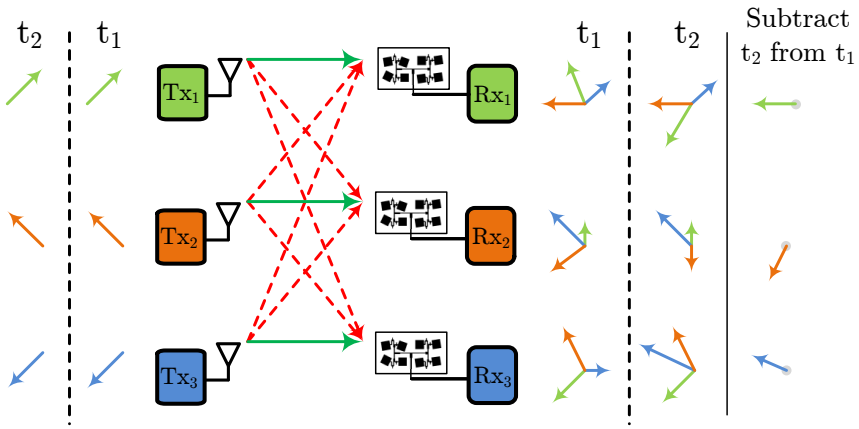

Fig. 3: A 3-user IC in which receivers are equipped with the proposed structure each with $M = 8$ sub-elements. Encoding and decoding of this example are discussed in Section III-D.

III. Transmission Strategy

A. Encoding strategy

We consider the problem of data transmission in an unknown time variant channel. We assume that each transmitter uses a digital modulation scheme in which Q different symbols can be

transmitted through selecting a single symbol from a set of $\mathcal{S} = \{S_1, S_2, \ldots, S_Q\}$. As an example for FSK modulation, we have:

$$U_i(t) = A\cos\left(2\pi(f_c + (i-1)\Delta f)t\right),\ 0 \le t \le T_s,\ 1 \le i \le Q, \tag{4}$$

where f_c indicates modulation frequency, T_s is the symbol duration and $\Delta f = f_j - f_{j-1}$. By considering $\mathcal{E}$ as the energy of each symbol, the parameter A is equivalent to $\sqrt{\frac{2\mathcal{E}}{T_s}}$.

We assume symbols (or messages) are uniformly distributed. Transmitter TX_i wishes to send uniformly distributed message $W^{[i]} \in \mathcal{W}^{[i]}$ to RX_i, $i \in \mathcal{K}$, over n uses of the channel with time duration of nT_s. The transmission rate for the above digital modulation technique can be calculated from the following relation:

$$R^{[i]} = \frac{\log_2 Q}{T_s},\ |\mathcal{W}^{[i]}| = 2^{nR^{[i]}}. \tag{5}$$

We assume that the messages at all the transmitters are independent from each other and the channel gains. Each transmitter is subject to the total average transmission power constraint of $P_t = \frac{\mathcal{E}}{T_s}$. Transmitter TX_i encodes its message $W^{[i]}$ using the encoding function $X^{[i]}(t) = e_i\left(W^{[i]}\right)$ where $i \in \mathcal{K}$ and $e_i\left(W^{[i]}\right)$ is an one to one function from messages to the stream of symbols at TX_i. In more simple notation we have the following relation:

$$X^{[i]}(t) = e_i\left(W^{[i]}\right) = \sum_j U_{i_j}\left(t - jT_s\right),\ 1 \le i_j \le Q \tag{6}$$

where $U_{i_j}\left(t - jT_s\right)$ represents transmission symbol in j^{th} transmission time.

Definition 1: We define the transmission block of $B_i, i \in \{1, \ldots, n\}$ in which all transmitters repeat their transmission symbols 2 times. Therefore the total transmission time of each block is $2T_s$ and for k^{th} transmitter we can assume that $U_{k_1} = U_{k_2}$. Therefore, in this case the transmission rate of equation 5 can be calculated as $R^{[i]} = \frac{\log Q}{2T_s}$.

B. Received Signal Model:

The output of each of the encoder functions from different transmitters is sent through a channel that has unknown impulse response at different sub-elements of the receiver antennas, and the noise power is added to the received signal. Thus, the received signal depends on the state of the switches at RX_i as given by:

$$Y^{[i]}(t) = \sum_{k\in\mathcal{K}}\sum_{m=1}^{M} s_m^{[i]} h_{mk}^{[i]}(t) X^{[k]}(t) + Z^{[i]}(t), 1 \le m \le M,\ s_m^{[i]} \in \{0,1\} \tag{7}$$

where $s_m^{[i]}$ represents the state of the m^{th} RF switch, $\mathcal{K}$ indicates the subset of active transmitters at B^{th} transmission block and $h_{mk}^{[i]}(t)$ shows channel coefficient between TX_k, and m^{th} subelement of the receiver antenna at $\text{RX}^{[i]}$. For simplicity of notation, we can define the channel coefficient vector as follows:

$$\bar{\mathbf{H}}^{[ik]} = \left[h_{1k}^{[i]}, h_{2k}^{[i]}, \ldots, h_{Mk}^{[i]}\right], \ k \in \mathcal{K}. \tag{8}$$

C. Decoding Strategy:

We assume that each receiver RX_i is aware of its channel state information and decodes its intended message $W^{[i]} \in \mathcal{W}^{[i]}$ using the decoding function $\hat{W}^{[i]} = \phi_i\left(\bar{\mathbf{Y}}^{[i]}, \text{SI}_{\text{Rx}_i}\right)$, where SI_{Rx_i} is the side information available to the receiver (in this case CSI). Then, the decoding error probability at receiver RX_i is given by

$$\lambda_e^{[i]}(n) = \sum_{W^{[i]} \in \mathcal{W}^{[i]}} P\left(W^{[i]}\right) \Pr\left(\hat{W}^{[i]} \neq W^{[i]}\right) = \mathbb{E}\left[\Pr\left(\hat{W}^{[i]} \neq W^{[i]}\right)\right], \tag{9}$$

where the expectation is over the random choice of messages. At the end of each block, all of the receivers have access to channel gains of $h_{mk}^{[j]}, 1 \leq m \leq M, k \in \mathcal{K}$. At the end of training signal transmission phase, all the receivers by the aid of a searching algorithm find two different reception states, $S^{[j]}(i_1)$ and $S^{[j]}(i_2)$, such that they satisfy the following conditions at RX_j:

$$\sum_{k \in \mathcal{K}} |\sum_{m=1}^{M} s_m^{[j]}(i_1) h_{mk}^{[j]} - \sum_{m=1}^{M} s_m^{[j]}(i_2) h_{mk}^{[j]}| \leq \delta, \ k \neq j \tag{10}$$

$$|\sum_{m=1}^{M} s_m^{[j]}(i_1) h_{mj}^{[j]} - \sum_{m=1}^{M} s_m^{[j]}(i_2) h_{mj}^{[j]}| \geq \Delta_j, \tag{11}$$

where (10) indicates that all the cross links in the two separate states of $S^{[j]}(i_1)$ and $S^{[j]}(i_2)$ have the same value to within a small value δ. Relation (11) indicates that the difference of all the direct links in two separate state of $S^{[j]}(i_1)$ and $S^{[j]}(i_2)$ is greater than Δ. When $\left(\frac{\Delta_j}{\delta}\right)^2$ has larger value, the portion of desired signal power to the interference signal power at RX_j has grater value. Both relations (10) and (11) can be expressed without subtraction equations as follows:

$$\sum_{k \in \mathcal{K}} |\sum_{m=1}^{M} \gamma_m^{[j]}(i_1) h_{mk}^{[j]}| \leq \delta, \ k \neq j \tag{12}$$

$$|\sum_{m=1}^{M} \gamma_m^{[j]} h_{mj}^{[j]}| \geq \Delta_j, \tag{13}$$

where $\gamma^{[j]} \in \{-1, 0, 1\}$. Therefore, we have 3^M different reception states to control the receiver antenna. Intuitively, if all the direct links change (the transmission link between TX_i and RX_i) and all the cross links (the transmission link between TX_i and $\mathrm{RX}_{i'}$ where $i \neq i'$) remain the same with the small value of δ, the receivers can decode their desired symbols by a simple subtraction of two sequential received signal at each block. We accomplish this goal by finding proper reception states using the proposed antenna structure.

D. 3-user example

Consider the 3-user interference channel of Fig. 3 to demonstrate how our antenna structure can help aligning most of interference signal power. In this example, we assume an antenna structure with $M = 8$ sub-elements, and we also assume all interfering channels have the same distribution of direct channel (we assume that distance of interference transmitters to the receiver is the same of desired transmitter to the receiver). Each transmitters repeats its signal across two time snapshots, and each antenna creates two observations in which the interfering signals remain (almost) the same and can be eliminated. The small grey circle in the last column of Figure 3 is the limit of interference residue.

As indicated in the table above, using a simple search algorithm among all $3^M = 6561$ combinations, we can drastically reduce the effect of interference signals. If all transmitters in this case use the same transmission power and the total additive noise power is negligible, we achieve the total signal to interference power of SINR as indicated in the table.

Fig. 4 shows the achievable rates of different schemes when all the transmitters have the same power. In this figure, the blue dotted line is the performance of treating-interference-as-noise (TIN). Since all transmitters have the same power, TIN is not a suitable solution here. The red dashed line is the achievable rate of an orthogonalization strategy such as TDMA and is equivalent to the capacity of a single point-to-point channel. Finally, the solid black curve corresponds to our transmission and reception strategy with the switching states indicated in the first table. Thus, for a wide operation SNR range, our protocol significantly outperforms the other schemes. As we discuss later in Section V-B, our gains saturate at high SNR.

E. Further Assumptions

Let λ denote the wavelength of the signal. At each receiver antenna structure, sub-elements are placed at least a minimum distance of $\frac{\lambda}{2}$ from their neighbours to have channel values which

TABLE I: Example of 3-user IC with $M = 8$ sub-elements at the receivers.

Channel vectors $\bar{\mathbf{H}}^{[ij]},\ i,j \in \mathcal{K},\ P_t = 30dB, P_n = 0dB$	$\gamma^{[i]} = s^{[i]}(i_1) - s^{[i]}(i_2)$	$10\log_{10}\left(\frac{\Delta_j}{\delta}\right)^2$
$\bar{\mathbf{H}}^{[11]} = [+0.5377, +1.8339, -2.2588, +0.8622, +0.3188, -1.3077, -0.4336, +0.3426]$	$\bar{\gamma}^{[1]} = (-1, 0, -1, 1, 1, -1, 0, -1)$	53 dB,
$\bar{\mathbf{H}}^{[12]} = [-1.3499, +3.0349, +0.7254, -0.0631, +0.7147, -0.2050, -0.1241, +1.4897]$		SINR =30 dB
$\bar{\mathbf{H}}^{[13]} = [+0.6715, -1.2075, +0.7172, +1.6302, +0.4889, +1.0347, +0.7269, -0.3034]$		
$\bar{\mathbf{H}}^{[21]} = [-1.1480, +0.1049, +0.7223, +2.5855, -0.6669, +0.1873, -0.0825, -1.9330]$		
$\bar{\mathbf{H}}^{[22]} = [+0.8404, -0.8880, +0.1001, -0.5445, +0.3035, -0.6003, +0.4900, +0.7394]$	$\bar{\gamma}^{[2]} = (-1, 1, 0, 0, -1, 1, 1, 1)$	22 dB,
$\bar{\mathbf{H}}^{[23]} = [-2.1384, -0.8396, +1.3546, -1.0722, +0.9610, +0.1240, +1.4367, -1.9609]$		SINR=21 dB
$\bar{\mathbf{H}}^{[31]} = [-1.0891, +0.0326, +0.5525, +1.1006, +1.5442, +0.0859, -1.4916, -0.7423]$		
$\bar{\mathbf{H}}^{[32]} = [-0.6156, +0.7481, -0.1924, +0.8886, -0.7648, -1.4023, -1.4224, +0.4882]$		31 dB,
$\bar{\mathbf{H}}^{[33]} = [+1.4193, +0.2916, +0.1978, +1.5877, -0.8045, +0.6966, +0.8351, -0.2437]$	$\bar{\gamma}^{[3]} = (1, 1, 1, 1, 0, 1, 0, 1)$	SINR=27 dB

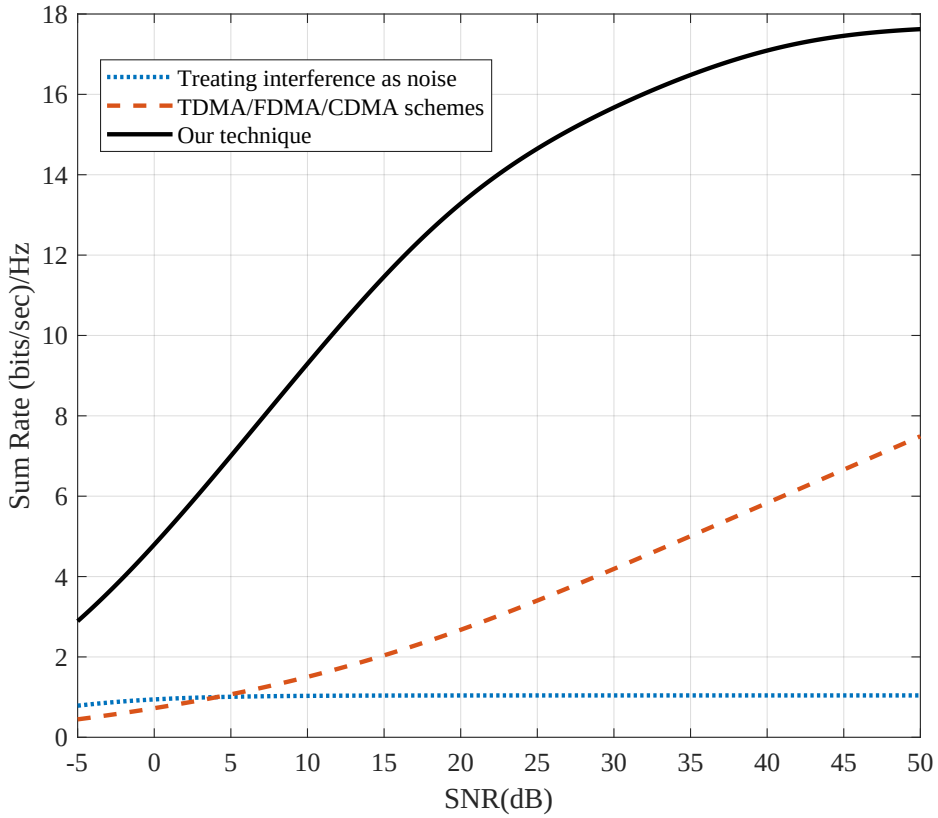

Fig. 4: A simple comparison among different transmission schemes with channel coefficient which is represented in the first table.

are independent. Therefore, we can assume that all the channel values of $h_{mk}^{[i]}(t)$ are independent

of each other and at each receiver, we have $K \times M$ different channel coefficients which are independent. In this paper, we assume cellular communication network with frequency reuse factor of $N = i^2 + ij + j^2,\ i, j \in \mathbb{W}^2$ in which each receiver is affected by many interference signals. In this case, the distance of the closest interfering transmitter to the center of each cell can be calculated from the following equation [22]:

$$D = R\sqrt{3N}, \tag{14}$$

wherein the above equation the value of R indicates the radius of each cell. The minimum ratio of the desired signal to the interference signal power from one interference signal can be calculated as follows:

$$\text{SIR} = \left(\frac{D}{R}\right)^{\alpha} = (3N)^{\frac{\alpha}{2}}, \tag{15}$$

wherein the above relations α represents path loss exponent in which for the free space environment has the value of 2 and for the more practical cases has a value greater than 2. As an example for the urban area this parameter will be 3 and for much more dense areas is 4.

IV. Motivation and Overview of the Contributions

Before presenting the results in great details, in this section, we provide a brief motivation and overview of our contributions. This paper provides answers to the following topics:

1) **Is there a contradiction with prior results?** It is known that the asymptotic high-SNR performance of interference channels, measured in terms of degrees-of-freedom, collapses to that of no channel knowledge if *perfect* channel state information is not available at the transmitters [23]. However, in this paper, we claim to attain the promised gains of IA, not only in the finite-SNR regime but also when no CSI is available at the transmitters. Thus, at first glance, there seems to be a contradiction. The reason why are results does not contradict any prior work is as follows. It is important to realize that degrees-of-freedom analysis does not necessarily inform us of the finite-SNR behaviour of wireless networks. As we see in the first thrust, using our proposed passive receive antenna design, we are able to provide the full benefit of IA within some *operational* SNR range, and beyond some threshold, our gains saturate. In other words, our results are in fact in agreement with the statement that in terms of degrees-of-freedom, no gain is obtained when CSI is missing, but for real-world SNR values, we can indeed provide

[2]Whole numbers or non-negative integers

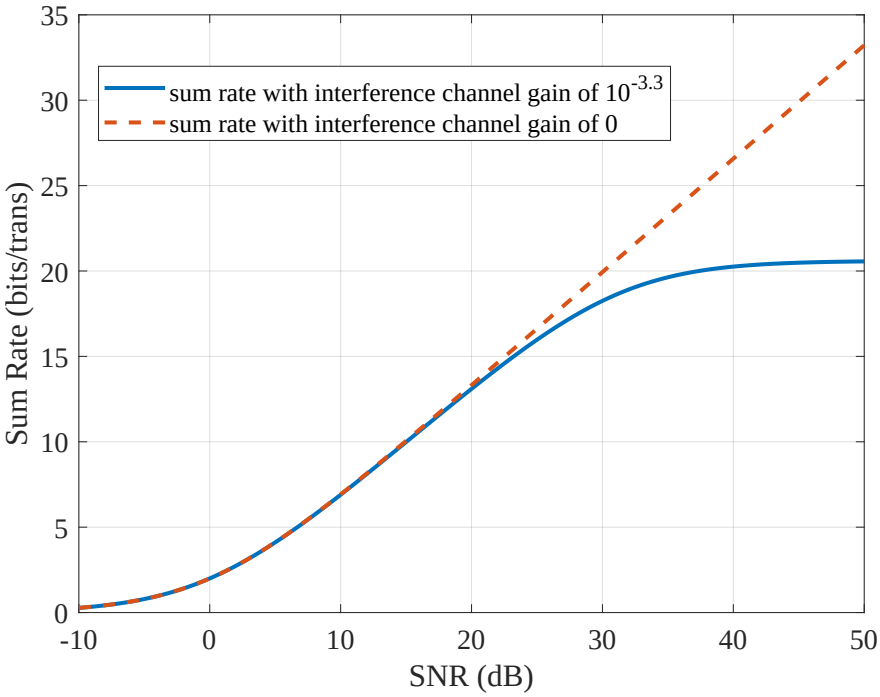

Fig. 5: Simple comparison between the achievable rate with perfect alignment and an imperfect alignment scheme. The solid curve shows the achievable sum DoF of zero while the dashed line shows perfect alignment scheme with sum DoF of 2 for 2-user interference channel, as it is indicated for the practical SNR region the imperfect alignment scheme trace the sum rate of perfect alignment scheme closely.

significant gains.

2) **Is DoF a proper metric to measure the performance of real wireless networks?** Although the DoF parameter can measure the performance of wireless networks in high SNR region, it cannot demonstrate the performance of wireless networks at applicable SNR regions. As an example consider $K-$user interference channel in which at each receiver the value of total interference signal power for all interference transmitters is a portion of desired signal power ($P_I = G_I P_d$), in this case, the total transmission rate treating interference as noise for per one reception dimension can be calculated as follows:

$$\begin{aligned} R_t\left(P_d/N\right) &= \frac{K}{2}\log_2\left(1+\frac{P_d}{N+P_I}\right) \\ &= \frac{K}{2}\log_2\left(1+\frac{P_d}{N+G_I P_d}\right). \end{aligned} \tag{16}$$

In which P_d is the desired signal power and P_I is the total interference signal power at each receiver. In this case, the value of sum DoF (d_{sum}) can be calculated as follows:

$$d_{\mathrm{sum}} = \lim_{P_d/N \to \infty} \frac{R_t\left(P_d/N\right)}{\log_2\left(P_d/N\right)} = 0, \tag{17}$$

while d_{sum} equals to zero, for low values of α we can trace the sum rate of $K/2\log_2\left(1+P_d/N\right)$ for wide range of P_d. Figure 5 compares the sum rate of $K=4$ user interference channel (sum DoF of 2) with not perfect interference cancellation scheme with $G_I = 10^{-3.3}$. As it is indicated in this figure, we can fully trace the curve of perfect interference alignment scheme for wide and applicable ranges of SNR.

3) **Is it possible to reach the benefit of IA without accessing CSIT?** In this paper, we propose an antenna structure in which the receivers can control the reception channel gain from the environmental signals and find the proper state using a searching algorithm. With the aid of this antenna structure without accessing channel state information at transmitters, the receivers can control the interference signals and align most of interference signal power.

4) **How does our solution compare to joint processing structures?** It is well known that using the structure of multiple antenna at the receiver can cancel the effect of interference signals from the environment but this antenna structure needs multiple RF chains and joint processing which is very sensitive to applying proper coefficients at each RF branch. Joint processing is needed at receivers which leads to higher hardware complexity. Our propose antenna structure only needs to use a simple antenna with some RF switches to control the interference signal power at the receiver. Also, it doesn't need joint processing at receiver and uses only one RF chain which reduces the price of deployment in any application.

V. Number of sub-elements vs. transmission rates

In this section, we evaluate the minimum number of sub-elements in our antenna structure to guarantee $\frac{\Delta^2}{\delta^2}$ is large enough for successful decoding at the receivers. The minimum number of required receiver elements and the switching modes is a function of $\delta_{\max}$ and the channel variance of σ_H^2. The channel variance parameter of σ_H^2 can be calculated from the following relation:

$$\sigma_H^2 = \int_{-\infty}^{\infty} h^2 f_H(h) dh, \tag{18}$$

wherein the above equation h is the channel value and $f_H(h)$ represents channel distribution. For simplicity of our analysis, we consider the real-valued base-band channel model. Then, we generalize the results to complex channel values.

We first present the following lemma which plays an important role in our analysis.

Lemma 1: If $\bar{\mathbf{H}}^{[ij]}$ *is the channel vector between* TX_j *and* RX_i*, then, for vector* $\bar{\gamma}^{[i]}$ *with elements in* $\{-1, 0, 1\}$*, the value of* $\bar{\mathbf{H}}^{[ij]}.\gamma^{[i]}$ *has the following average variance:*

$$\bar{\mathrm{var}}\left(\bar{\mathbf{H}}^{[ij]}.\bar{\gamma}^{[i]}\right) = \frac{M}{2}\sigma_H^2 \triangleq V \tag{19}$$

where $\bar{\mathbf{H}}^{[ij]}.\bar{\gamma}^{[i]}$ *is the inner product between two vectors of* $\bar{\mathbf{H}}^{[ij]}$ *and* $\gamma^{[i]}$ *of the same size.*

Proof: The vector $\bar{\gamma}^{[i]} = \left(\gamma_1^{[i]}, \ldots, \gamma_M^{[i]}\right)$ has 3^M different shapes in which $\gamma_k^{[i]} \in \{-1, 0, 1\}$. The inner product of two vectors $\bar{\mathbf{H}}^{[ij]}$ and $\bar{\gamma}^{[i]}$ can be expanded as follows:

$$\bar{\mathbf{H}}^{[ij]}.\bar{\gamma}^{[i]} = \sum_{k=1}^{M} h_k^{[ij]}\gamma_k^{[j]}. \tag{20}$$

Therefore, we have:

$$\mathrm{var}\left(\bar{\mathbf{H}}^{[ij]}.\bar{\gamma}^{[i]}\right) = \mathrm{var}\left(\sum_{k=1}^{M} h_k^{[ij]}\gamma_k^{[i]}\right) \tag{21}$$

$$= \sum_{k=1}^{M} \mathrm{var}\left(h_k^{[ij]}\right)|\gamma_k^{[i]}| = \sigma_H^2 \sum_{k=1}^{M} |\gamma_k^{[i]}| \tag{22}$$

If we consider uniform distribution among different state of the vector $\bar{\gamma}^{[i]}$, the average variance of $\mathrm{var}\left(\bar{\mathbf{H}}^{[ij]}.\bar{\gamma}^{[i]}\right)$ can be calculated as follows:

$$\bar{\mathrm{var}}\left(\bar{\mathbf{H}}^{[ij]}.\bar{\gamma}^{[i]}\right) = \mathbb{E}\left(\sigma_H^2 \sum_{k=1}^{M} |\gamma_k^{[i]}|\right) \tag{23}$$

$$= \sigma_H^2 \sum_{l=0}^{M} p\left(\sum_{k=1}^{M} |\gamma_k^{[i]}| = l\right) l,\ 0 \le l \le M. \tag{24}$$

If we consider uniform distribution among different switching states, the value of $p\left(\sum_{k=1}^{M} |\gamma_k^{[i]}| = l\right)$ can be calculated from $\frac{\binom{M}{M-l}}{2^M}$. In which, the value of $\binom{M}{M-l}$ counts the number of states in which the vector $\bar{\gamma}^{[i]}$ contains $M - l$ zeros and 2^M indicates total number of states for $|\bar{\gamma}^{[i]}|$ which contains zero or one. Therefore, we can conclude that:

$$\bar{\mathrm{var}}\left(\bar{\mathbf{H}}^{[ij]}.\bar{\gamma}^{[i]}\right) = \frac{\sum_{l=0}^{M}\binom{M}{M-l}l}{2^M}\sigma_H^2, \tag{25}$$

if we substitute $M - l$ with l', then:

$$\bar{\mathrm{var}}\left(\bar{\mathbf{H}}^{[ij]}.\bar{\gamma}^{[i]}\right) = \frac{\sum_{l'=0}^{M}\binom{M}{l'}(M - l')}{2^M}\sigma_H^2 = \frac{M}{2}\sigma_H^2 \tag{26}$$

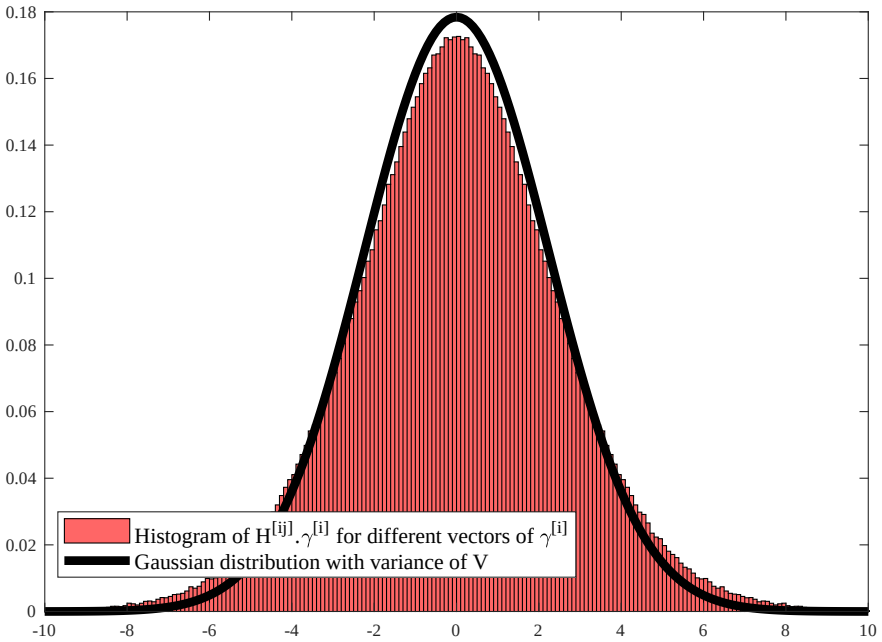

Fig. 6: Simple comparison between Gaussian distribution with zero mean and variance of $V = \frac{\sum_{l=0}^{M}\binom{M}{l}(M-l)}{2^M}\sigma_H^2$ and distribution of $\bar{\mathbf{H}}^{[ij]}.\bar{\gamma}^{[i]}$ for different $\bar{\gamma}^{[i]}$'s.

which completes the proof. ■

The distribution of $\bar{\mathbf{H}}^{[ij]}.\bar{\gamma}^{[i]}$ has a symmetric bell shape. A simple histogram of this parameter with $M = 10$ is plotted in Fig. 7. This distribution can be approximated with zero mean Gaussian distribution with similar variance.

Lemma 2: For small enough positive values of δ, the probability of finding a vector $\bar{\gamma}^{[i]}$ to satisfy $|\bar{\mathbf{H}}^{[ij]}.\bar{\gamma}^{[i]}| < \delta$ can be approximated by $\frac{2}{\sqrt{2\pi}}\frac{\delta}{V} - \frac{2}{3\sqrt{2\pi}}\frac{\delta^3}{V^3} + O\left(\frac{\delta^5}{V^5}\right)$ for $\sigma = \sqrt{V}$ where V is defined in (19).

Proof: As it discussed in the previous lemma for different vectors, $\bar{\gamma}^{[i]}$, the distribution of $\bar{\mathbf{H}}^{[ij]}.\bar{\gamma}^{[i]}$ can be approximated by Gaussian distribution with zero mean and variance V. So, we have:

$$p\left(|\bar{\mathbf{H}}^{[ij]}.\bar{\gamma}^{[i]}| < \delta\right) = \int_{-\delta}^{\delta} \frac{1}{\sqrt{2\pi V}} e^{-\frac{r^2}{2V}} dr \tag{27}$$

$$\overset{(a)}{\approx} \int_{-\delta}^{\delta} \frac{1}{\sqrt{2\pi V}} \left(1 - \frac{r^2}{2V} + O\left(\frac{r^4}{V^3}\right)\right) dr \tag{28}$$

$$= \frac{2}{\sqrt{2\pi}}\frac{\delta}{\sigma} - \frac{2}{3\sqrt{2\pi}}\frac{\delta^3}{\sigma^3} + O\left(\frac{\delta^5}{\sigma^5}\right) \tag{29}$$

where the approximation (a) comes from the Taylor series expansion of the term $e^{-\frac{r^2}{2V}}$ and in all the above equations σ is equal to $\sqrt{V}$. ■

Since δ is small, we can ignore the effect higher order terms of $\frac{\delta}{\sigma}$. Therefore, we can assume that:

$$p\left(|\bar{\mathbf{H}}^{[ij]}.\bar{\gamma}^{[i]}| < \delta\right) \approx \frac{2}{\sqrt{2\pi}}\frac{\delta}{\sigma} = \frac{2}{\sqrt{\pi M}}\frac{\delta}{\sigma_H}. \tag{30}$$

Therefore, in this case the probability of finding two different switching states of $S^{[i]}(k_1)$ and $S^{[i]}(k_2)$ at RX_i in which the values of $\sum_{m=1}^{M} s_m^{[i]}(k_1)h_{mj}^{[i]}$ and $\sum_{m=1}^{M} s_m^{[i]}(k_2)h_{mj}^{[i]}$ are within the value of $\delta_{\max}$ can be approximated as follows:

$$p\left(|\bar{\mathbf{H}}^{[ij]}.\bar{\gamma}^{[i]}| < \delta_{\max}\right) \approx \frac{2}{\sqrt{\pi M}}\frac{\delta_{\max}}{\sigma_H},\ i \text{ is constant} \tag{31}$$

The probability of satisfying the above condition for all the cross links at RX_i in the active set of $\mathcal{K}$ can be approximated as follows:

$$p\left(|\bar{\mathbf{H}}^{[ij]}.\bar{\gamma}^{[i]}| < \delta_{\max}\right) \approx \left(\frac{2}{\sqrt{\pi M}}\frac{\delta_{\max}}{\sigma_H}\right)^{|\mathcal{K}|-1}, j \in \mathcal{K}. \tag{32}$$

A. Determining the minimum required number of sub-elements M

In this subsection, using the previous lemmas, we determine the minimum number of antenna sub-elements to satisfies our interference alignment scheme within a maximum threshold of $\delta_{\max}$. In other words, we find M such that almost surely we have $|\bar{\mathbf{H}}^{[ij]}.\bar{\gamma}^{[i]}| < \delta_{\max}$.

Lemma 3: The minimum number of M to almost surely satisfy $|\bar{\mathbf{H}}^{[ij]}.\bar{\gamma}^{[i]}| < \delta_{\max}$ is

$$\frac{|\mathcal{K}|-1}{\log 3}\log\left(\frac{\sigma_H}{\delta_{\max}}\right) + c, \tag{33}$$

where c is a function of M and for practical scenarios not greater than 1.5.

Proof: We have 3^M different reception states. In order to, with high probability, align interference signal power at RX_j, *i.e.* satisfy (12) and (13) with high probability, we need:

$$3^M\left(\frac{2}{\sqrt{\pi M}}\frac{\delta_{\max}}{\sigma_H}\right)^{|\mathcal{K}|-1} > 1, \tag{34}$$

resulting in

$$M > \frac{|\mathcal{K}|-1}{\log 3}\log\left(\frac{\sqrt{\pi M}\sigma_H}{2\delta_{\max}}\right). \tag{35}$$

In particular, if $M \leq 32$ (due to practical limits), we can relax the right hand-side of the above inequality as $M > \frac{|\mathcal{K}|-1}{\log 3}\log\left(\frac{\sigma_H}{\delta_{\max}}\right) + 1.5$. We can conclude that all each receiver should have a

minimum number of $\left\lceil \frac{|\mathcal{K}|-1}{\log 3} \log\left(\frac{\sigma_H}{\delta_{\max}}\right) + 1.5 \right\rceil$ elements to align interference signals within the value of $\delta^2_{\max}$. ■

We can rearrange (35) to obtain a bound on $\delta_{\max}$ based on the number of sub-elements:

$$\delta_{\max} < 2^{-\frac{M-1.5}{|\mathcal{K}|-1}\log 3}\sigma_H. \tag{36}$$

Example: As an example consider we have $|\mathcal{K}| = 4$ active transmitters and assume that $\delta_{\max} = 0.1$ and $\sigma_H^2 = 1$. In this case, the minimum number of sub-elements in the receiver antenna structure (M) equals to 8. We note that in a cellular network, we typically expect interference from a small number of nearby base-stations and $|\mathcal{K}| = 4$ is a reasonable assumption.

B. Average achievable sum-rate

Denote the (physical) distance from transmitter TX_j to RX_k with d_{kj}. Then, the average achievable sum-rate can be calculated by treating as noise the total remaining interference power after the decoding strategy as follows:

$$C^{[k]}_{\text{avg}} = \int_{-\infty}^{+\infty} \frac{1}{4}\log\left(1 + \frac{\delta^2 P_t/d_{kk}^{\alpha}}{P_n + \delta^2_{\max}\left(\sum_j \frac{1}{d_{kj}^{\alpha}}\right)P_t}\right) f_{\Delta}(\delta)d\delta, j \neq k, j \in \mathcal{K} \tag{37}$$

where α is the path loss exponent coefficient, P_n is additive noise power, and from the first lemma $f_{\Delta}(\delta)$ is Gaussian distribution with zero mean and the variance of $\frac{M}{2}\sigma_H^2$. The coefficient $\frac{1}{4}$ comes from the transmission in two time snapshots and the basic coefficient of channel capacity for point to point communication. For a cellular communication network, we can substitute d_{kk} and d_{kj} with R and $R\sqrt{3N}$, respectively where R is the maximum cell radios and $R\sqrt{3N}$ is interference signal distance from the receiver. So, we can change the above equality with the following inequality:

$$C^{[k]}_{\text{avg}} \geq \int_{-\infty}^{+\infty} \frac{1}{4}\log\left(1 + \frac{\delta^2 P_t/R^{\alpha}}{P_n + \delta^2_{\max}\left(\sum_j \frac{1}{(R\sqrt{3N})^{\alpha}}\right)P_t}\right) f_{\Delta}(\delta)d\delta,\ j \neq k, j \in \mathcal{K}. \tag{38}$$

If all interfering transmitters have the same distance to the receiver, and $P_t >> P_n$, then the above inequality can be simplified as follows:

$$C^{[k]}_{\text{avg}} \geq \int_{-\infty}^{+\infty} \frac{1}{4}\log\left(1 + \frac{\delta^2 P_t/R^{\alpha}}{P_n + \delta^2_{\max}\left(\frac{|\mathcal{K}-1|}{(R\sqrt{3N})^{\alpha}}\right)P_t}\right) f_{\Delta}(\delta)d\delta,\ j \neq k, j \in \mathcal{K}. \tag{39}$$

$$\overset{(a)}{\approx} \int_{-\infty}^{+\infty} \frac{1}{4}\log\left(\frac{\delta^2(3N)^{\frac{\alpha}{2}}}{\delta^2_{\max}(|\mathcal{K}|-1)}\right) f_{\Delta}(\delta)d\delta \tag{40}$$

$$= \int_{-\infty}^{+\infty} \frac{1}{4}\log\left(\delta^2\right) f_{\Delta}(\delta)d\delta + \frac{1}{4}\log\left(\frac{(3N)^{\frac{\alpha}{2}}}{\delta^2_{\max}(|\mathcal{K}|-1)}\right), \tag{41}$$

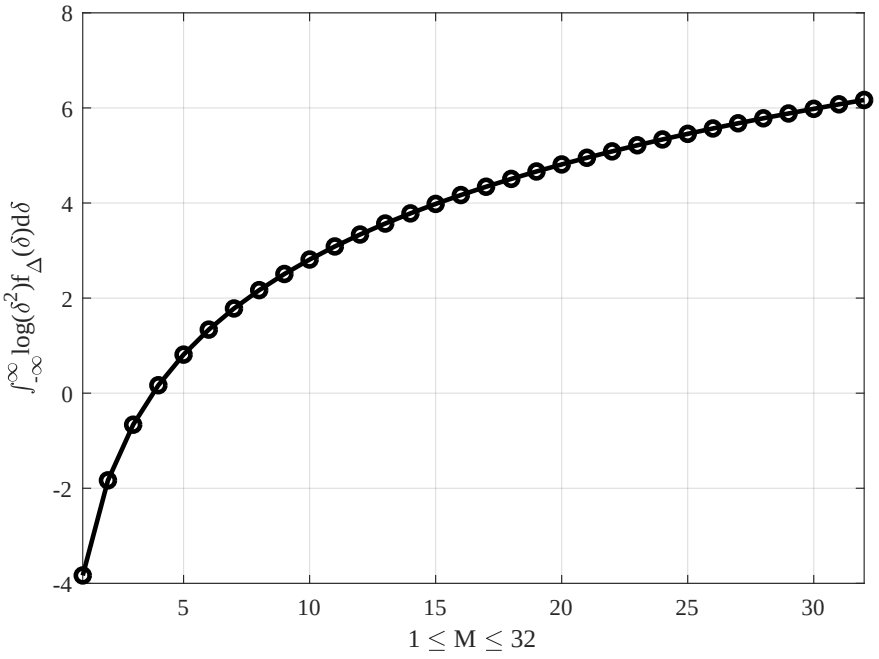

Fig. 7: The numerical value of $\int_{-\infty}^{+\infty} \log(\delta^2) f_\Delta(\delta) d\delta$ for different values of the number of sub-elements $1 \leq M \leq 32$.

where (a) comes from the assumption that $P_t >> P_n$.

Remark 2: Here, we make the assumption that $P_t >> P_n$ in order to simplify the expression for the saturation point (the point beyond which we do not follow the pre-log factor of $K/2$), and obtain some insights as we discuss below. The motivation for this assumption is that at saturation point, interference power is the main bottleneck for communications.

From the above equations and (36) where $\delta_{\max} < 2^{-\frac{M-1.5}{|\mathcal{K}|-1} \log 3} \sigma_H$, we can conclude that:

$$C_{\text{avg}}^{[k]} \geq \int_{-\infty}^{+\infty} \frac{1}{4} \log\left(\delta^2\right) f_\Delta(\delta) d\delta + \frac{M-1.5}{2(|\mathcal{K}|-1)} \log 3 + \frac{\alpha}{8} \log 3N - \frac{1}{4} \log\left((|\mathcal{K}|-1)\sigma_H\right), \quad (42)$$

considering $\sigma_H = 1$ the total average capacity of C_{avg} can be lower bounded by $|\mathcal{K}| C_{\text{avg}}^{[k]}$ as follows:

$$C_{\text{avg}} \geq \int_{-\infty}^{+\infty} \frac{|\mathcal{K}|}{4} \log\left(\delta^2\right) f_\Delta(\delta) d\delta + \frac{M-1.5}{2} \log 3 + \frac{\alpha|\mathcal{K}|}{8} \log 3N - \frac{|\mathcal{K}|}{4} \log\left(|\mathcal{K}|-1\right) \quad (43)$$

In the above lower-bound, we have four terms that can be interpreted as follows:

- $\int_{-\infty}^{+\infty} \frac{|\mathcal{K}|}{4} \log(\delta^2) f_\delta(\delta) d\delta$: This term captures the multi-path gain of the environment at the antenna, see Fig. 7. We note that with beamforming, such gains would disappear;

- $\frac{M-1.5}{2}\log 3$: This term indicates the rate that can be achieved from the number of antenna sub-elements. It is interesting that without having multi-channel processing (*i.e.* joint processing), we still obtain the benefit multi-channel processing from the new proposed antenna structure with only one RF chain. The term $\frac{\log 3}{2}$ in this relation comes from having three different states for each sub-element across two times;
- $\frac{\alpha|\mathcal{K}|}{8}\log 3N$: This term indicates the rate achieved through the path-loss exponent and the frequency reuse factor which can help the receivers reduce the effect of of interference signals;
- $-\frac{|\mathcal{K}|}{4}\log\left(|\mathcal{K}|-1\right)$: This term represents the negative impact of interfering signals in the transmission environment which reduces the chance of finding proper channel condition at the receivers.

C. Outage capacity analysis

In this subsection, we analyze the outage capacity of our technique for different values of P_t. We define $(1-\epsilon)$ outage capacity for each user as follows:

$$C_{1-\epsilon}=\left\{R_t : P\left(R_t \geq C_h\right)\geq 1-\epsilon\right\}, \tag{44}$$

where R_t is the transmission rate in which there exist a state among $\frac{3^M-1}{2}$ different states with channel capacity of C_h with the probability greater than $1-\epsilon$. If we assume Gaussian distribution for $f_\Delta(\delta)$ with variance of $\frac{M}{2}\sigma_H^2$, the outage capacity can be calculated as follows:

$$C_{1-\epsilon}=\frac{1}{4}\log\left(1+\frac{\Delta_\epsilon^2 P_t/R^\alpha}{P_n+\delta_{\max}^2\left(\frac{|\mathcal{K}-1|}{(R\sqrt{3N})^\alpha}P_t\right)}\right), \tag{45}$$

where Δ_ϵ is a positive-valued Δ for which $1-\int_{-\Delta_\epsilon}^{\Delta_\epsilon} f_\Delta(\delta)d\delta \geq 1-\epsilon$. From the first lemma, if we consider Gaussian distribution with variance $\frac{M}{2}\sigma_H^2$ for $f_\Delta(\delta)$, the value of Δ_ϵ for specific value of ϵ can be calculated using the inverse of Q-function as follows:

$$\Delta_\epsilon=\sqrt{\frac{M}{2}}\sigma_H Q^{-1}\left(\frac{1-\epsilon}{2}\right). \tag{46}$$

VI. Search Algorithm

In the previous section, we proved that using our antenna structure it is possible to (almost surely) create conditions to align most of interference signal power to within a small value $\delta_{\max}$. In order to materialize this scheme, we need to search among 3^M different reception sates to

find the best switching state at each receiver. For cellular wireless network applications, we typically engage with not more than 3 interference signals and choosing $M = 8$ is sufficient for our results. Therefore, in this small practical case, our scheme can be implemented using a brute-force search algorithm to go through $\frac{3^8-1}{2} = 3280$ points to minimize the effect of interference signals and maximize the desired signal power. However, when networks are dense and we engage with more users, the brute-force search becomes impractical.

Before we discuss our search algorithm, we define the optimization problem this algorithm needs to solve. From our system model and definitions, let $\bar{\gamma}^{[i]} = \left(\gamma_1^{[i]}, \gamma_2^{[i]}, \ldots, \gamma_M^{[i]}\right)$ be a vector where $\gamma_j^{[i]} \in \{-1, 0, 1\}$. At RX_i, the goal is to:

$$\max_{\bar{\gamma}^{[i]}} |h_{1i}^{[i]}\gamma_1^{[i]} + h_{2i}^{[1]}\gamma_2^{[i]} + \ldots h_{Mi}^{[i]}\gamma_M^{[i]}|, \tag{47}$$

while

$$|h_{1j}^{[i]}\gamma_1^{[i]} + h_{2j}^{[i]}\gamma_2^{[i]} + \cdots + h_{Mj}^{[i]}\gamma_M^{[i]}| \leq \delta_j, \;\; j \neq i, j \in \mathcal{K}, \tag{48}$$

where δ_j is a small positive real number. Another representation of this problem is as follows:

$$\max_{\bar{\gamma}^{[i]}} \frac{|\bar{\gamma}^{[i]}.\bar{\mathbf{H}}^{[ii]}|}{\sum_{j\in\mathcal{K}} |\bar{\gamma}^{[i]}.\bar{\mathbf{H}}^{[ij]}|}, \tag{49}$$

where in the above equation $\mathbf{U}.\mathbf{H}^{[i]}$ is the inner product between two vectors $\mathbf{U}$ and $\mathbf{H}^{[i]}$. We refer to

$$\frac{|\bar{\gamma}^{[i]}.\bar{\mathbf{H}}^{[ii]}|}{\sum_{j\in\mathcal{K}} |\bar{\gamma}^{[i]}.\bar{\mathbf{H}}^{[ij]}|} \tag{50}$$

as the *score function*.

Next, $\mathbf{H}^{[i]}$ can be expanded as follows:

$$\mathbf{H}^{[i]} = \left(h_1^{[i]}, h_2^{[i]}, \ldots, h_M^{[i]}\right). \tag{51}$$

It is straightforward to see that a simple brute-force search algorithm has a complexity of $\frac{3^M-1}{2}$, where the division by 2 comes from the fact that if $\bar{\gamma}_*^{[i]}$ is the optimum vector (except all-zero vector which is not a solution) for our optimization problem, then $-\bar{\gamma}_*^{[i]}$ is also an optimum vector. For large values of M, a brute-force search algorithm would be hard to implement.

A. Proposed search algorithm:

We propose a state search method in which all switching states of the i^{th} receiver generate a set $\Gamma^{[i]} = \{\gamma_1^{[i]}, \gamma_2^{[i]}, \ldots, \gamma_M^{[i]}\},\ \gamma_j^{[i]} \in \{-1, 0, 1\}$. Our search algorithm is based on following steps:

Step1: We generate $\binom{M}{L}$ different sates[3] of $\mathcal{F}_r^{[i]}, 1 \leq r \leq \binom{M}{L}$ where each state represents a set in which $|\mathcal{F}_r^{[i]}| = L$ and $\mathcal{F}_r \subset \Gamma^{[i]}$.

Step2: At the first stage, each time using a simple brute-force search algorithm, we calculate the *score function* for different subsets of $\mathcal{F}_r^{(1)},\ 1 \leq r \leq \binom{M}{L}$ and we select N_s survived states (parents) with highest *score functions*. We call them survived subsets of $\{\mathcal{FS}_1^{(1)}, \mathcal{FS}_2^{(1)}, \ldots, \mathcal{FS}_{N_s}^{(1)}\}$ from the first stage. The complexity of this step is $3^L\binom{M}{L}$.

Note: When we calculate the *score function* for each state, we set all other elements in the set $\Gamma^{[i]} \setminus \mathcal{F}_r$ to be zero.

Step 3: For every survived subset, we generate new subsets of $\mathcal{F}_r^{(2)},\ 1 \leq r \leq \binom{M-L}{L}$ from the remaining members of $\Gamma^{[i]} \setminus \mathcal{FS}_r^{(1)}$ which we refer to as the offsprings of the parents from the previous stage. Similar to previous step, we choose N_s of them with highest *score function* as new parents and survived subsets.

Step 4: We repeat step 3 until no subsets are left.

Fig 8 shows our proposed searching algorithm to find a (possibly locally optimal) vector $\bar{\gamma}^{[i]}$ to maximize our *score function*.

B. Complexity of the proposed search algorithm:

As we discussed earlier, a simple brute-force search algorithm needs $\frac{3^M-1}{2}$ searching points to find the optimum solution. In this subsection, we analyze the complexity of our proposed search algorithm. At the first stage, we need to search among $\binom{M}{L}$ subsets where each subset using a simple brute-force algorithm needs to search among $\frac{3^L-1}{2}$ searching points. Therefore, at the first step we have a complexity of $\frac{3^L-1}{2}\binom{M}{L}$. At the second stage, we have N_s survived parents where for each parent we need to generate $\binom{M-L}{L}$ subsets. Similar to the previous stage, we need to search among $\frac{3^L-1}{2}$ searching point. Therefore, in this stage, we have a complexity of $N_s\frac{3^L-1}{2}\binom{M-L}{L}$. In general, during the i^{th} stage, we have the following complexity:

$$N_s\frac{3^L-1}{2}\binom{M-(i-1)L}{L}. \tag{52}$$

[3]We assume M is divisible by L.

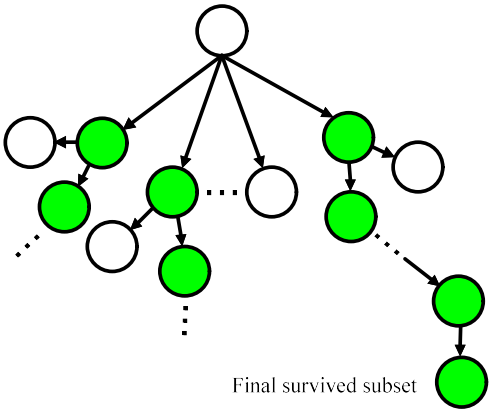

Fig. 8: The coloured nodes indicate survived subsets and selected parents to generate children, among generated children in each stage we survived L of them with the highest score function to generate the next parents.

Finally, during the last stage, we have a complexity of $\frac{3^L-1}{2}$ (there is no choice to select among the subsets). Therefore, the total complexity of our algorithm can be calculated as follows:

$$\sum_{i=1}^{\frac{M}{L}-1} N_s \frac{3^L-1}{2} \binom{M-(i-1)L}{L} + \frac{3^L-1}{2}. \tag{53}$$

As an example, for $M = 32$, $L = 2$, and $N_s = 5$, the complexity of our proposed search algorithm at each receiver is 57104 which is 1.6×10^{10} times faster than the simple brute-force search algorithm.

As another example, consider a 3-user interference channel in which the channel vectors at the first receiver has the following form:

$$\bar{\mathbf{H}}^{[11]} = [+1.4090, +1.4172, +0.6715, -1.2075, +0.7172, +1.6302], \tag{54}$$

$$\bar{\mathbf{H}}^{[12]} = [+0.4889, +1.0347, +0.7269, -0.3034, +0.2939, -0.7873], \tag{55}$$

$$\bar{\mathbf{H}}^{[13]} = [+0.8884, -1.1471, -1.0689, -0.8095, -2.9443, 1.4384]. \tag{56}$$

Using the brute-force search algorithm with complexity of $3^6 = 729$ and setting $\bar{\gamma}^{[1]} = (-1, 1, 0, 1, -1, 0)$, we can reach a *score function* of $\frac{\Delta^2}{\delta^2} = 293.5$. Now, we want to test our proposed search algorithm

by setting $N_s = 2$ and $L = 2$. In this case, the first receiver generate $\binom{6}{2} = 15$ subsets as follows:

$$\begin{aligned}
&\mathcal{F}_1^{[1]} = \{\gamma_1^{[1]}, \gamma_2^{[1]}\},\ \mathcal{F}_2^{[1]} = \{\gamma_1^{[1]}, \gamma_3^{[1]}\},\ \mathcal{F}_3^{[1]} = \{\gamma_1^{[1]}, \gamma_4^{[1]}\} \\
&\mathcal{F}_4^{[1]} = \{\gamma_1^{[1]}, \gamma_5^{[1]}\},\ \mathcal{F}_5^{[1]} = \{\gamma_1^{[1]}, \gamma_6^{[1]}\},\ \mathcal{F}_6^{[1]} = \{\gamma_2^{[1]}, \gamma_3^{[1]}\} \\
&\mathcal{F}_7^{[1]} = \{\gamma_2^{[1]}, \gamma_4^{[1]}\},\ \mathcal{F}_8^{[1]} = \{\gamma_2^{[1]}, \gamma_5^{[1]}\},\ \mathcal{F}_9^{[1]} = \{\gamma_3^{[1]}, \gamma_4^{[1]}\} \\
&\mathcal{F}_{10}^{[1]} = \{\gamma_2^{[1]}, \gamma_6^{[1]}\},\ \mathcal{F}_{11}^{[1]} = \{\gamma_3^{[1]}, \gamma_5^{[1]}\},\ \mathcal{F}_{12}^{[1]} = \{\gamma_3^{[1]}, \gamma_6^{[1]}\} \\
&\mathcal{F}_{13}^{[1]} = \{\gamma_4^{[1]}, \gamma_5^{[1]}\},\ \mathcal{F}_{14}^{[1]} = \{\gamma_4^{[1]}, \gamma_6^{[1]}\},\ \mathcal{F}_{15}^{[1]} = \{\gamma_5^{[1]}, \gamma_6^{[1]}\}.
\end{aligned} \tag{57}$$

For each subset above, using a simple brute-force search algorithm the receiver maximizes the *score function* $f\left(\mathcal{F}_j^{[1]}\right), 1 \leq j \leq \binom{6}{2} = 15$, and finds $N_s = 2$ of them with highest *score function*. In the above example the maximum score function for each of the above subset can be calculated as follows:

$$\begin{aligned}
&f\left(\mathcal{F}_1^{[1]}\right) = 3.3444, (-1,-1,0,0,0,0),\ f\left(\mathcal{F}_2^{[1]}\right) = 2.8651, (-1,0,-1,0,0,0), \\
&f\left(\mathcal{F}_3^{[1]}\right) = 1.9510, (0,0,0,-1,0,0),\ f\left(\mathcal{F}_4^{[1]}\right) = 1.9307, (-1,0,0,0,0,0), \\
&f\left(\mathcal{F}_5^{[1]}\right) = 1.9307, (-1,0,0,0,0,0),\ f\left(\mathcal{F}_6^{[1]}\right) = 5.5135, (0,-1,1,0,0,0), \\
&f\left(\mathcal{F}_7^{[1]}\right) = 3.6173, (0,-1,0,1,0,0),\ f\left(\mathcal{F}_8^{[1]}\right) = 0.8416, (0,-1,0,0,0,0), \\
&f\left(\mathcal{F}_9^{[1]}\right) = 63.580, (0,-1,0,0,0,-1),\ f\left(\mathcal{F}_{10}^{[1]}\right) = 3.1278, (0,0,-1,1,0,0), \\
&f\left(\mathcal{F}_{11}^{[1]}\right) = 0.2699, (0,0,-1,0,0,0),\ f\left(\mathcal{F}_{12}^{[1]}\right) = 37.7934, (0,0,-1,0,0,-1) \\
&f\left(\mathcal{F}_{13}^{[1]}\right) = 1.9510, (0,0,0,-1,0,0),\ f\left(\mathcal{F}_{14}^{[1]}\right) = 1.9510, (0,0,0,-1,0,0), \\
&f\left(\mathcal{F}_{15}^{[1]}\right) = 2.1943, (0,0,0,0,-1,-1).
\end{aligned} \tag{58}$$

Given $N_s = 2$, $f\left(\mathcal{F}_9^{[1]}\right) = 63.580, \bar{\gamma}^{[1]} = (0,-1,0,0,0,-1)$ and $f\left(\mathcal{F}_{12}^{[1]}\right) = 37.7934, \bar{\gamma}^{[1]} = (0,0,-1,0,0,-1)$ are the survived parents. From the first survived state $\mathcal{FS}_9^{[1]} = (0,-1,0,0,0,-1)$, we have $\binom{6-N_s}{2} = 6,\ N_s = 2$ offspings as follows:

$$\begin{aligned}
&f\left(\mathcal{F}_1^{[1]}\right) = 63.58, (0,-1,0,0,0,-1),\ f\left(\mathcal{F}_2^{[1]}\right) = 165.4732, (1,-1,0,1,0,-1), \\
&f\left(\mathcal{F}_3^{[1]}\right) = 63.58, (0,-1,0,0,0,-1),\ f\left(\mathcal{F}_4^{[1]}\right) = 63.58, (0,-1,0,0,0,-1), \\
&f\left(\mathcal{F}_5^{[1]}\right) = 63.58, (0,-1,0,0,0,-1),\ f\left(\mathcal{F}_6^{[1]}\right) = 63.58, (0,-1,0,0,0,-1).
\end{aligned} \tag{59}$$

From the survived state $\mathcal{FS}_{12}^{[1]} = (0, 0, -1, 0, 0, -1)$, we have $\binom{6-N_s}{2} = 6,\ N_s = 2$ offsprings as follows:

$$f\left(\mathcal{F}_1^{[1]}\right) = 37.7934, (0, 0, -1, 0, 0, -1),\ f\left(\mathcal{F}_2^{[1]}\right) = 37.7934, (0, 0, -1, 0, 0, -1),$$
$$f\left(\mathcal{F}_3^{[1]}\right) = 37.7934, (0, 0, -1, 0, 0, -1),\ f\left(\mathcal{F}_4^{[1]}\right) = 37.7934, (0, 0, -1, 0, 0, -1),$$
$$f\left(\mathcal{F}_5^{[1]}\right) = 37.7934, (0, 0, -1, 0, 0, -1),\ f\left(\mathcal{F}_6^{[1]}\right) = 37.7934, (0, 0, -1, 0, 0, -1). \tag{60}$$

From the above relations, we can determine two further survived parents of $f\left(\mathcal{F}_2^{[1]}\right) = 165.4732$, $\bar{\gamma}^{[1]} = (1, -1, 0, 1, 0, -1)$ and $f\left(\mathcal{F}_1^{[1]}\right) = 63.58, \bar{\gamma}^{[1]} = (0, -1, 0, 0, 0, -1)$ where each parent has one offspring. Finally, the *score function* is maximized by setting $\bar{\gamma}_*^{[1]} = (1, -1, 0, 1, 0, -1)$ and the value of *score function* is 165.4732 with a complexity of 256 compared to $3^6 = 729$ for the brute-force algorithm. The gap between our proposed algorithm and the brute-force algorithm grows quickly as M increases.

C. Random search:

In this case, we randomly choose different $\bar{\gamma}^{[i]}$'s at each receiver and we select a vector which satisfies the minimum SINR condition at that receiver. When the value of M is large enough, we will show in the numerical results that the number of local maximums is sufficiently large to satisfy our conditions.

VII. Numerical and simulation results

In this section, we numerically analyze the performance of our proposed alignment strategy using our antenna structure. In our simulation results, we assume Rayleigh fading channels in which the real and the imaginary parts of the channel gains are modeled by independent and identically distributed zero-mean Gaussian processes. Since the real and the imaginary parts are independent of each other, our technique can be modified using simple 90 degrees phase shifter elements and RF switches. Therefore, we analyze only the real part of channel coefficients and the results can be generalized to complex channels. Basically, in all our simulations, we assume that there exist real-valued channel coefficients with Gaussian distribution among transmitters and receivers sub-elements.

Figure 9 shows a comparison between Monte Carlo simulation with 1000 tries and our approximation of relation (61), where we have:

$$p\left(|\bar{\mathbf{H}}^{[ij]}.\bar{\gamma}^{[j]}| < \delta\right) \approx \frac{2}{\sqrt{\pi M}} \frac{\delta_{\max}}{\sigma_H},\ j \text{ is constant.} \tag{61}$$

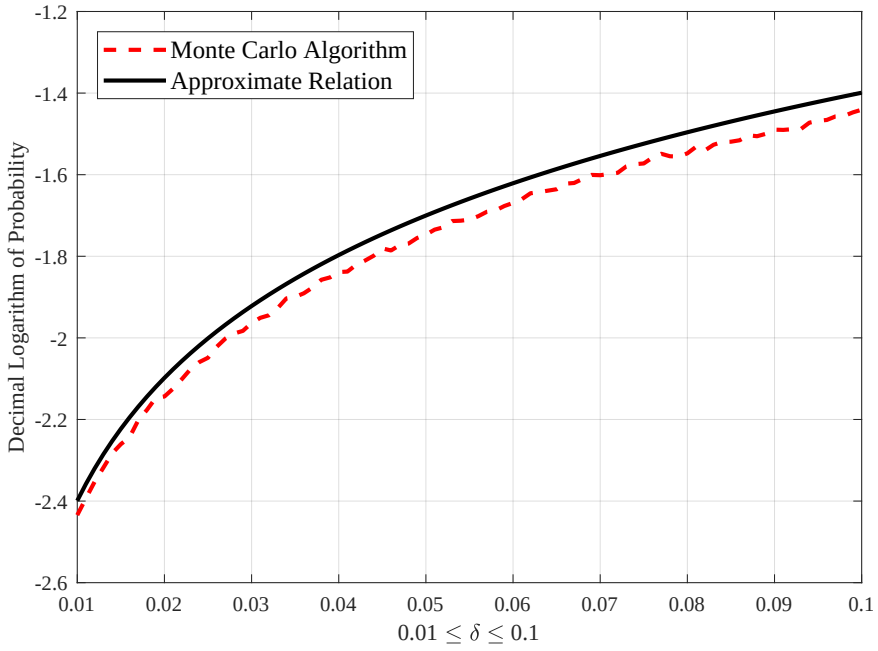

Fig. 9: The comparison between our approximation result of relation (61) and Monte Carlo simulation for $M = 8$, $\sigma_H = 1$, and 1000 tries.

We observe that our approximation traces the simulation results within a small margin when $0.01 \leq \delta \leq 0.1$. As it is indicated in this figure, our approximate relation becomes more accurate for smaller values of δ.

Figure 10 shows our average transmission rate for a 4-user interference channel with $M = 16$ sub-elements at each receiver. In this figure, the red solid curve indicates the sum rate of a $4-$user interference channel with perfect CSI, the dashed blue curve indicate the sum rate of this channel using our antenna structure and a simple brute-force algorithm. From (43), a lower-bound on the saturation rate can be calculated as follows:

$$C_{\text{avg}} \geq \int_{-\infty}^{+\infty} \frac{|\mathcal{K}|}{4} \log\left(\delta^2\right) f_{\Delta}(\delta) d\delta + \frac{M - 1.5}{2} \log 3 + \frac{\alpha|\mathcal{K}|}{8} \log 3N - \frac{|\mathcal{K}|}{4} \log\left(|\mathcal{K}| - 1\right) \tag{62}$$

$$= \frac{4 \times 4}{4} + \frac{16 - 1.5}{2} \log 3 - \frac{4}{4} \log 52 = 13.16, \tag{63}$$

which matches what we observe in Figure 10. We should note that since in this case we do not use the interference reduction technique of cellular networks, the term $\frac{\alpha|\mathcal{K}|}{8} \log 3N$ does not play a role in our relation (all the interference signals are received at the same power level).

As it is indicated our antenna structure can help the receivers to trace the sum rate of original IA scheme in applicable SNR region ($\text{SNR} \leq 40\text{dB}$) without accessing channel state information at

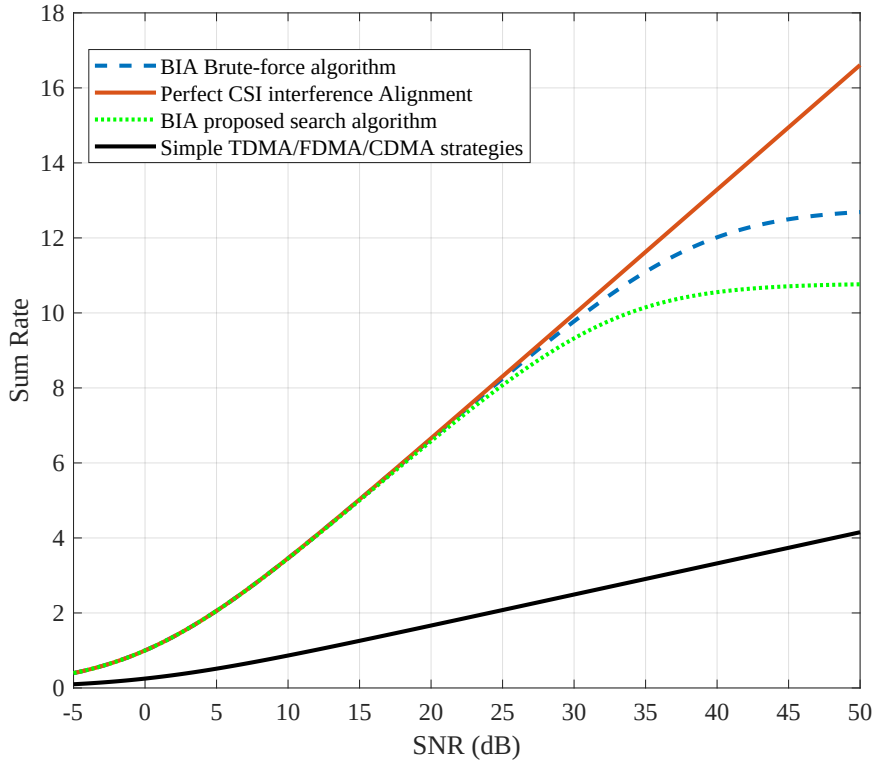

Fig. 10: The comparison between our proposed strategy and the perfect CSI alignment technique in 4-user IC.

transmitters. Since the simple brute-force increases complexity at receivers we use our proposed searching algorithm, as it is indicated in Fig. 10 by use of $N_s = 2$ and $L = 4$ with the complexity of 1.8×10^4 compared to brute-force search with the complexity of 2.15×10^7 we have a little back-off in order of 5 dB which still completely practical and good to be used. We observe that using our technique, the perfect interference alignment sum-rate outer-bound is traced for a wide range of SNR values. We note that the perfect interference alignment scheme works for high SNR values and the bound is included for comparison.

Figure 11 shows the outage capacity of our proposed strategy for different values of $1 - \epsilon$. Not surprisingly, when $\epsilon = 0$, we cannot find any value for R_t (transmission rate) in which the receiver can almost surely recover the transmitted data. Therefore, in this case, the value of $C_{1-\epsilon}$ is zero. As ϵ moves away from zero, the value of $C_{1-\epsilon}$ starts increasing.

Table II and III show the performance and complexity of our proposed search algorithm compared to random search algorithm with complexity of $\frac{3^8-1}{2}$ and simple brute-force algorithm. For $K = 4$ users, our approach exhibits good performance while reducing the complexity of

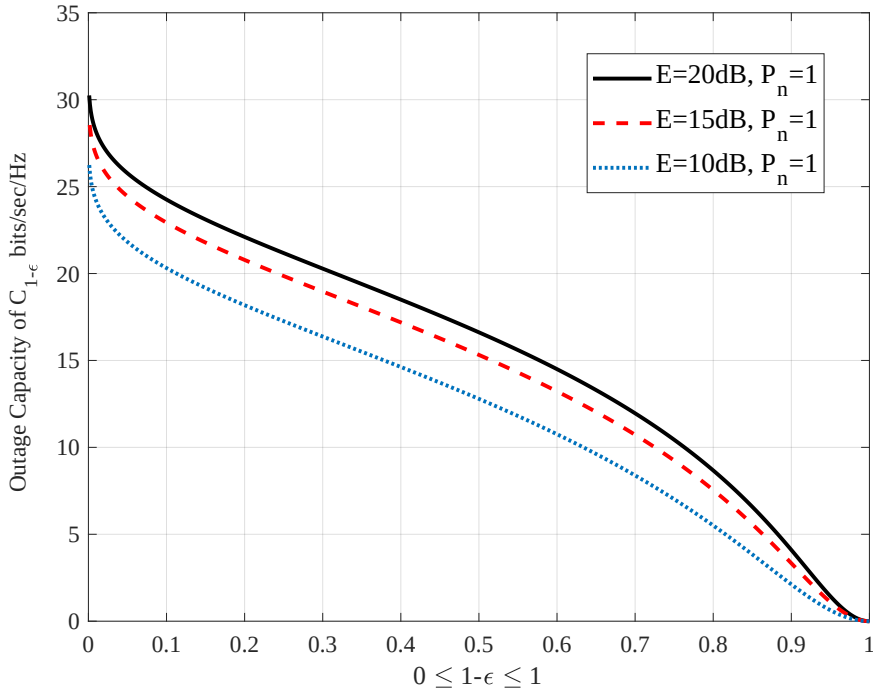

Fig. 11: The outage capacity as a function of $1-\epsilon$ for $M=12$ sub-elements and $K=6$ users and different values of transmission power ($\mathcal{E}=10,15,20\text{dB}$).

TABLE II: Example of 4-user IC and the highest *score function* value

K=4	$M=8$	$M=16$	$M=24$
Brute-force algorithm	$\max \frac{\Delta^2}{\delta^2}=100$	$\max \frac{\Delta^2}{\delta^2}=16\times 10^4$	$\max \frac{\Delta^2}{\delta^2}=9\times 10^6$
Proposed strategy	$\max \frac{\Delta^2}{\delta^2}=100$	$\max \frac{\Delta^2}{\delta^2}=7.5\times 10^4$	$\max \frac{\Delta^2}{\delta^2}=3\times 10^6$
Random search	$\max \frac{\Delta^2}{\delta^2}=100$	$\max \frac{\Delta^2}{\delta^2}=3\times 10^3$	$\max \frac{\Delta^2}{\delta^2}=8\times 10^4$

search algorithm drastically. For $M=16$, our sum rate has a saturation point around 48dB and has a complexity of 19000 which even with basic processors at 60MHz can be calculated within 0.3ms. Considering channel coherence time of 6.25ms for a receiver with a speed of 30m/sec and operation frequency of 1.6GHz, the search algorithm overhead is a negligible part of signaling.

VIII. Conclusion and Future Work

In this paper, we considered the feasibility of interference alignment in $K-$user ICs without accessing CSI at the transmitters. We proposed a new antenna structure with several sub-elements

TABLE III: Complexity of different schemes compared to our scheme with $L = 4$ and $N_s = 2$

K=4	$M = 8$	$M = 16$	$M = 24$
Brute-force algorithm	$\frac{3^8-1}{2}$	$\frac{3^{16}-1}{2}$	$\frac{3^{24}-1}{2}$
Proposed strategy	5640	1.9×10^4	1.4×10^6
Random search	$\frac{3^8-1}{2}$	$\frac{3^8-1}{2}$	$\frac{3^8-1}{2}$

each controlled by an RF switch. One of the most important differences of this antenna structure with other similar multiple antenna structures is that it can be used without using joint processing at the receivers and multiple RF chains. The proposed scheme allows transceivers to achieve higher average sum-rate without accessing CSI at the transmitters matching the promised gains of Interference Alignment for finite SNR values. We designed our scheme such that interference signals align to within a small margin. We showed that when the number of sub-elements at the receivers increases, the chance of finding proper channel conditions to eliminate most of interfering signal power increases. We then analyzed the average achievable sum-rate of our approach, and we proposed an efficient algorithm to search among different reception states. We showed that by a small sacrifice in SINR, we can find proper states with lower complexity. Through numerical analysis, we showed that our new approach enables interference mitigating without the main drawbacks of prior results. One can extend the results of this paper for other types of interference channels and channel networks with different topology or protocols to improve data reception rate which is the main bottleneck in today wireless networks. Another step to improve the performance of the system is to analyze the antenna structure with different types of antenna sub-elements or increase the number of reception switching state with some phase shifter or attenuator elements. It is obvious by increasing the number of reception states the chance of finding proper switching state at receivers increases and we expect better performance.

REFERENCES

[1] A. E. Gamal and M. Costa, "The capacity region of a class of deterministic interference channels," *IEEE Transactions on Information Theory*, vol. 28, pp. 343–346, March 1982.

[2] R. Etkin, D. Tse, and H. Wang, "Gaussian interference channel capacity to within one bit," *IEEE Transactions on Information Theory*, vol. 54, pp. 5534–5562, December 2008.

[3] A. Vahid, M. Maddah-Ali, and A. S. Avestimehr, "Capacity results for binary fading interference channels with delayed CSIT," *IEEE Transactions on Information Theory*, vol. 60, no. 10, pp. 6093–6130, 2014.

[4] Te Han and K. Kobayashi, "A new achievable rate region for the interference channel," *IEEE Transactions on Information Theory*, vol. 27, pp. 49–60, January 1981.

[5] A. El Gamal and Y.-H. Kim, *Network information theory*. Cambridge university press, 2011.

[6] T. S. Rappaport, G. R. MacCartney, M. K. Samimi, and S. Sun, "Wideband millimeter-wave propagation measurements and channel models for future wireless communication system design," *IEEE Transactions on Communications*, vol. 63, pp. 3029–3056, Sep. 2015.

[7] S. W. Choi, S. A. Jafar, and S.-Y. Chung, "On the beamforming design for efficient interference alignment," *IEEE Communications Letters*, vol. 13, no. 11, pp. 847–849, 2009.

[8] M. Johnny and M. R. Aref, "An efficient precoder size for interference alignment of the K-user interference channel," *IEEE Communications Letters*, vol. 21, no. 9, pp. 1941–1944, 2017.

[9] B. Nosrat-Makouei, J. G. Andrews, and R. W. Heath, "Mimo interference alignment over correlated channels with imperfect csi," *IEEE Transactions on Signal Processing*, vol. 59, pp. 2783–2794, June 2011.

[10] M. A. Maddah-Ali and D. N. Tse, "Completely stale transmitter channel state information is still very useful," *IEEE Transactions on Information Theory*, vol. 58, pp. 4418–4431, July 2012.

[11] H. Maleki, S. A. Jafar, and S. Shamai, "Retrospective interference alignment over interference networks," *IEEE Journal of Selected Topics in Signal Processing*, vol. 6.3, pp. 228–240, June 2012.

[12] A. Vahid, M. A. Maddah-Ali, and A. S. Avestimehr, "Approximate capacity region of the miso broadcast channels with delayed CSIT," *IEEE Transactions on Communications*, vol. 64, no. 7, pp. 2913–2924, 2016.

[13] D. Castanheira, A. Silva, and A. Gameiro, "Retrospective interference alignment: Degrees of freedom scaling with distributed transmitters," *IEEE Transactions on Information Theory*, vol. 63, pp. 1721–1730, March 2017.

[14] A. Vahid, M. A. Maddah-Ali, and A. S. Avestimehr, "Capacity results for binary fading interference channels with delayed CSIT," *IEEE Transactions on Information Theory*, vol. 60, no. 10, pp. 6093–6130, 2014.

[15] S. A. Jafar, "Blind interference alignment," *IEEE Journal of Selected Topics in Signal Processing*, vol. 6, no. 3, pp. 216–227, 2012.

[16] M. Johnny and M. R. Aref, "Bia for the k-user interference channel using reconfigurable antenna at receivers," *IEEE Transactions on Information Theory*, vol. 66, pp. 2184–2197, April 2020.

[17] G. Caire and S. Shamai, "On achievable rates in a multi-antenna gaussian broadcast channel," in *Proceedings. 2001 IEEE International Symposium on Information Theory (IEEE Cat. No.01CH37252)*, pp. 147–, June 2001.

[18] S. A. Jafar, "Too much mobility limits the capacity of wireless ad hoc networks," *IEEE Transactions on Information Theory*, vol. 51, pp. 3954–3965, Nov 2005.

[19] T. Gou, C. Wang, and S. A. Jafar, "Aiming perfectly in the dark-blind interference alignment through staggered antenna switching," *IEEE Transactions on Signal Processing*, vol. 59, pp. 2734–2744, June 2011.

[20] M. Johnny and M. R. Aref, "Sum degrees of freedom for the k-user interference channel using antenna switching," in *WSA 2017; 21th International ITG Workshop on Smart Antennas*, pp. 1–6, March 2017.

[21] A. Vahid and M. Johnny, "Low-complexity practical implementation of blind interference alignment using reconfigurable antennas," *U.S. Patent no. 62,888,697*, Aug 2019.

[22] T. S. Rappaport *et al.*, *Wireless communications: principles and practice*, vol. 2. prentice hall PTR New Jersey, 1996.

[23] A. G. Davoodi and S. A. Jafar, "Aligned image sets under channel uncertainty: Settling conjectures on the collapse of degrees of freedom under finite precision CSIT," *IEEE Transactions on Information Theory*, vol. 62, no. 10, pp. 5603–5618, 2016.